

## Distribution of Transmissible Amyloid Proteins in the Liver with Apolipoprotein A-II Amyloidosis

Yingye LIU<sup>1)</sup>, Jinko SAWASHITA<sup>1)2)</sup>, Yaoyong WANG<sup>1)3)</sup>, Lin LI<sup>1)</sup>, Hiroki MIYAHARA<sup>1)</sup>  
Xin DING<sup>1)</sup>, Mu YANG<sup>1)</sup> and Keiichi HIGUCHI<sup>1)2)\*</sup>

- 1) *Department of Aging Biology, Institute of Pathogenesis and Disease Prevention, Shinshu University Graduate School of Medicine*
- 2) *Department of Biomedical Sciences for Intractable Neurological Diseases, Institute for Biomedical Sciences, Interdisciplinary Cluster for Cutting Edge Research, Shinshu University*
- 3) *Fenyang Hospital Affiliated with Shanxi Medical University, Shanxi, China*

In some amyloidoses, transmission by self-propagating amyloid proteins plays a critical role in the progression of the disease. Mouse senile amyloidosis is a disorder in which apolipoprotein A-II (ApoA-II) deposits as amyloid fibrils (AApoAII), and it might be transmitted by ingestion of those amyloid fibrils. Characterization of protein species responsible for transmission of mouse AApoAII amyloidosis should provide valuable information. Here, we studied the distributions of ApoA-II and inducing activities in liver fractions that were insoluble or soluble and had different degrees of amyloid deposition. ApoA-II was mainly contained in the 3,000 x g pellet fractions regardless of the degree of amyloid deposition. The 3,000 x g pellet fraction showed strong amyloid fibril-specific fluorescence of fibril-bound thioflavin T and strong amyloidosis-inducing activity. Sonication of liver homogenate increased the proportion of ApoA-II and inducing activity of the 100,000 x g pellet fraction. Weak inducing activity was found in the soluble fraction. We fractionated and isolated multiple assemblies of AApoAII amyloid fibrils by non-denaturing polyacrylamide gel electrophoresis. ApoA-II proteins ranging from monomers to large oligomers had low amyloidosis inducing activity. These results suggest that transmission of AApoAII amyloidosis may be primarily associated with the insoluble amyloid fibril structure. *Shinshu Med J 64 : 183–194, 2016*

(Received for publication February 9, 2016 ; accepted in revised form February 25, 2016)

---

**Key words :** mouse apolipoprotein A-II, insoluble fraction, multiple assemblies of proteins, thioflavin T, transmission of amyloidosis

---

**Abbreviations :** AApoAII, amyloid fibril of apolipoprotein A-II ;  $A\beta$ , amyloid  $\beta$  ; AD, Alzheimer's disease ; AI, amyloid index ; ApoA-II, apolipoprotein A-II ; AS, amyloid score ; DW, distilled water ; PAGE, polyacrylamide gel electrophoresis ; ThT, thioflavin T

### I Introduction

Amyloidosis refers to a group of diseases caused by structural disorders of proteins whereby nor-

mally soluble proteins are deposited in tissues as highly ordered, insoluble amyloid fibrils<sup>1)</sup>. Currently, over 30 amyloid fibril proteins are known to be associated with amyloidoses<sup>2)</sup>, including amyloid light chain amyloidosis, familial amyloid polyneuropathy and reactive amyloid A (AA) amyloidosis. These are characterized by amyloid deposition in multiple organs. In some types of amyloidosis, such as Alzheimer's disease (AD) and prion diseases, amyloid deposits are limited to the brain<sup>3)</sup>. Apolipo-

---

\* Corresponding author : Keiichi Higuchi  
Department of Aging Biology, Institute of Pathogenesis and Disease Prevention, Shinshu University Graduate School of Medicine, 3-1-1 Asahi, Matsumoto, Nagano 390-8621, Japan  
E-mail : keiichih@shinshu-u.ac.jp

protein A-II (ApoA-II) is the second most abundant apolipoprotein in plasma high-density lipoprotein (HDL) after apolipoprotein A-I but the physiological functions of ApoA-II are still unclear. The molecular weight of ApoA-II is 8.7 kDa. In mice, ApoA-II polymerizes into amyloid fibrils (AApoAII) and deposits systemically (except in the brain) as a function of age<sup>4)5)</sup>. Based on these findings, the amyloid fibrils of mouse senile amyloidosis were termed "AApoAII". AApoAII is present universally in aged mice of various strains. Moreover, a hereditary form has been found in humans<sup>6)</sup>. Intriguing recent studies have suggested that the aggregates of misfolded ApoA-II protein act as seeds that induce conversion of the native ApoA-II to fibrillar AApoAII assemblies. When young and amyloidosis-negative mice were injected with AApoAII amyloid fibrils extracted from various organs, feces or milk of amyloid-laden mice, AApoAII amyloidosis was readily induced<sup>7)8)</sup>. Thus, AApoAII amyloidosis could be transmitted through a mechanism similar to that of infectious prion diseases.

Infectious prions consist of multimers of prion proteins differing in size and solubility. They are resistant to proteinase K treatment and fragmentation by chemical or physical methods<sup>9)–12)</sup>. The most infectious units were reported to be much smaller than the fibrils<sup>13)</sup>. Similarly,  $A\beta$  species seem to contain small and large oligomers, protofibrils and fibrils<sup>14)</sup>. Furthermore, the sizes of the soluble pools consisting of small  $A\beta$  aggregates were found to correlate highly with the severity and progression of AD<sup>15)16)</sup>. It was found that the soluble and insoluble fractions differed in their induction of  $A\beta$ -amyloid deposition in a mouse model of AD, and small  $A\beta$  aggregates provided relatively more molecular interfaces to promote efficient propagation compared with large aggregates or fibrils<sup>17)</sup>. Sonication of large  $A\beta$  assemblies into numerous smaller seeds increased the infective activity<sup>18)</sup>.

Here, we investigated the distribution of ApoA-II among insoluble and soluble protein fractions from the livers of mice at different stages of amyloidosis. We also examined their abilities to transmit

amyloidosis. Furthermore, we fractionated isolated amyloid fibrils into multiple ApoA-II assemblies by non-denaturing polyacrylamide gel electrophoresis (PAGE). The fractions were then assessed for their amyloidosis-inducing activities. We selected the liver for our investigation for the following reasons. First, the liver has the most severe AApoAII amyloid deposition among organs and relatively large amounts of amyloid fibrils could be isolated from the liver. Second, intravenous injection of amyloid fibrils reproducibly induces amyloid deposition in the liver.

## II Materials and Methods

### A Animals

R1.P1-*Apoa2<sup>c</sup>* is a congenic strain of mice that has the amyloidogenic *c* allele of the ApoA-II gene (*Apoa2<sup>c</sup>*)<sup>5)</sup>. R1.P1-*Apoa2<sup>c</sup>* mice were maintained under specific pathogen-free conditions in the Division of Laboratory Animal Research, Department of Life Science, Research Center for Human and Environmental Science, Shinshu University. A commercial diet (MF; Oriental Yeast, Tokyo, Japan) and tap water were available *ad libitum*. All experiments were performed with the approval of the Committee for Animal Experiments of Shinshu University.

### B Induction and detection of AApoAII amyloid deposition

Amyloidosis was induced in 2-month-old female R1.P1-*Apoa2<sup>c</sup>* mice by intravenous injection of 100  $\mu$ g AApoAII fibrils. Two, 4, 7, 10, and 13 months after injection, the treated mice were killed and a part of the liver was removed and stored at  $-70^{\circ}\text{C}$ . Each organ was fixed in 10% neutral buffered formalin, embedded in paraffin and cut into serial 4- $\mu$ m sections for detection of amyloid deposition. Amyloid deposition was identified in Congo red-stained sections by polarizing microscopy. The intensity of the AApoAII deposition in each organ was determined using an amyloid score (AS) that was graded from 0 to 4: grade 0, no AApoAII; grade 1, a minute amount; grade 2, small amounts; grade 3, a moderate amount and grade 4, extensive

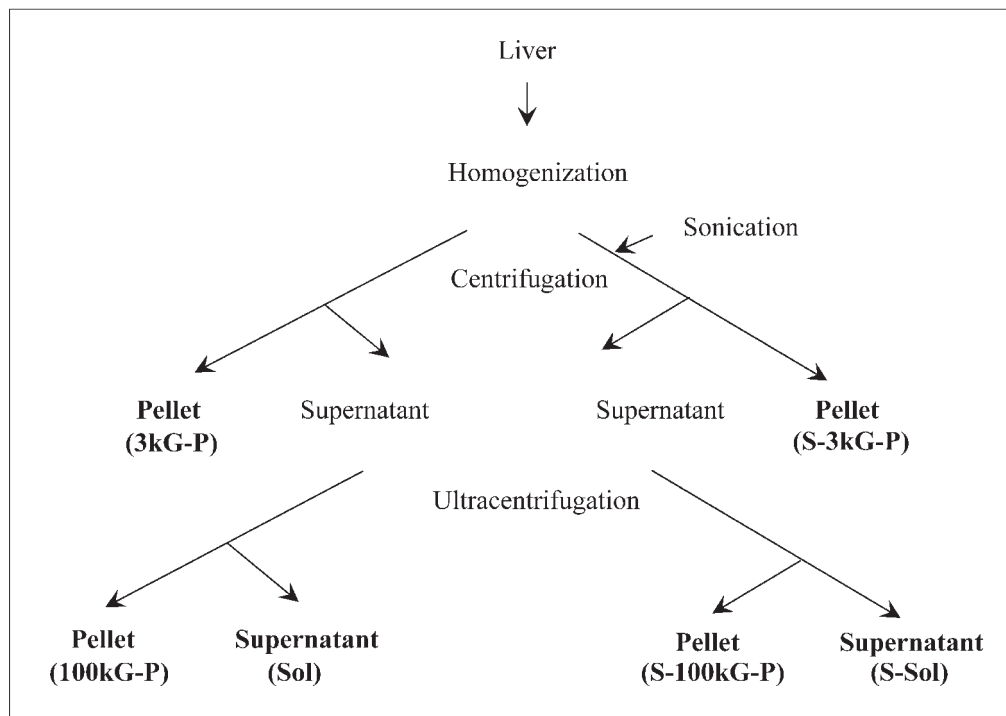


Fig. 1 Flow chart for extraction of insoluble and soluble ApoA-II fractions from the liver. Liver tissues in PBS were processed with a homogenizer. In some cases, the tissues were further sonicated on ice. Homogenates without or with sonication were centrifuged at 3,000  $\times$  g for 5 min at 4  $^{\circ}$ C. The pellets were re-suspended in PBS (3kG-P and S-3kG-P without and with sonication, respectively). The supernatants were centrifuged at 100,000  $\times$  g for 1 hr at 4  $^{\circ}$ C. The supernatants (Sol and S-Sol without and with sonication, respectively) and the pellets (100kG-P and S-100kG-P without and with sonication, respectively) were obtained for further analysis.

AApoAII deposits. More detailed criteria for each grade in each organ were described previously<sup>19</sup>. The amyloid index (AI) is the average of the AS scores in 7 organs (heart, liver, spleen, stomach, small intestine, tongue and skin) and a parameter of the degree of AApoAII deposition in the whole body. Amyloid fibrils were assayed by a thioflavin T (ThT) fluorometric method<sup>20</sup>.

### C Extraction of insoluble and soluble ApoA-II fractions from the liver

Liver tissue was homogenized in phosphate buffered saline (PBS) with a homogenizer (Power Masher, Nippi, Tokyo, Japan). In some cases, it was further sonicated 3 times on ice for 30 sec with an ultrasonic homogenizer VP-5S (Tietech Co, Ltd, Tokyo, Japan) at a power level of 4 at 30 sec intervals. The 3kG-P, 100kG-P, Sol, S-3kG-P, S-100kG-P and S-Sol fractions were obtained as shown in **Fig. 1**. The protein content of each fraction was

determined with the BCA assay (Pierce BCA Protein Assay Kit, Thermo Scientific, Tokyo, Japan).

### D Western blot and electron microscopic analysis

Fractions were analyzed on Tris-Tricine/SDS-16.5 % polyacrylamide gels (SDS-PAGE). After electrophoresis, the 6 protein fractions were transferred to polyvinylidene difluoride (PVDF) membranes using a semi-dry Western blot apparatus (Nihon Eido, Tokyo, Japan) at 150 mA for 1.5 hr. ApoA-II was detected with rabbit anti-ApoA-II antiserum<sup>21</sup> and the enhanced chemiluminescence method with X-ray film<sup>9</sup>. The density of the positive band of ApoA-II was quantitated using NIH Images Ver. 1.61. AApoAII fibrils were purified from the liver of mice with heavy amyloid depositions and were used as a standard to calculate the relative content of ApoA-II in the fractions. The negatively stained samples were observed with a

JEM-1400 (HC) electron microscope (JEOL, Tokyo, Japan)<sup>8)</sup>.

#### **E Fractionation and isolation of amyloid fibrils by non-denaturing PAGE**

Amyloid fibrils were isolated from livers 2, 4, 7, 10 and 13 months after induction of amyloidosis<sup>19)</sup>. AApoAII amyloid fibrils were separated into 5 fractions by non-denaturing PAGE as explained below. Amyloid fibrils in sample buffer (12 % glycerol, 62.5 mM Tris pH 6.8, 0.02 % bromophenol blue) were applied to premade non-denaturing 5-20 % PAGE gel (SDG-571, Bio Craft, Tokyo, Japan) and separated by electrophoresis in 25 mM Tris pH 8.3, 192 mM glycine running buffer with 0.01 % SDS at 2 mA for 20 hr. The non-denatured PAGE gels were cut into 5 fractions as follows: I, monomers and dimers (6-15 kDa); II, trimers, tetramers, and pentamers (15-49 kDa); III, small oligomers (49-82 kDa); IV, large oligomers (82-180 kDa), and V, ~fibrils (>180 kDa). The gels containing the 5 fractions were minced with scissors and homogenized 3 times in cold distilled water (DW) with a Polytron homogenizer for 30 sec with 30 sec intervals, and then fractions were ultracentrifuged at 100,000 x g for 1 hr at 4 °C. Supernatants were transferred to new tubes.

#### **F Transmission activities of the various fractions**

We assessed the amyloidosis-inducing activity of the 6 insoluble and soluble fractions of liver homogenates and the 5 fractions isolated from amyloid fibrils with non-denaturing PAGE gels. Thus, each fraction containing 10  $\mu$ g of ApoA-II was injected into the tail vein of three 2-month-old female R1.P1-*Apoa2<sup>c</sup>* mice. After 2 months, amyloid deposition was determined.

#### **G Immuno-depletion analysis of soluble fraction**

Protein G-Agarose beads were washed three times in PBS at room temperature and incubated for 60 min with 10  $\mu$ l of anti-ApoA-II antiserum or normal rabbit serum, then washed three times in PBS at 4 °C. The soluble (Sol) fraction of 7m-1 mouse was diluted to a final concentration of 1 mg/ml in DW. The diluted fractions were allowed to react with antibody-bead complexes overnight at 4 °

C. Then the mixture was centrifuged at 3,000 x g for 2 min at 4 °C, and the supernatants were harvested and used for transmission experiments. The pellet and supernatant were used for Western blotting with anti-ApoA-II antiserum to assess immuno-depletion.

#### **H Statistical analysis**

Because the AI value is a nonlinear index, the values from different groups of mice were compared by using the nonparametric Mann-Whitney U-test.

### **III Results**

#### **A Amyloid deposition induced with AApoAII amyloid fibril injection**

We injected AApoAII fibrils into 2-month-old female R1.P1-*Apoa2<sup>c</sup>* mice to induce amyloidosis. Two months after induction, amyloid deposition was detectable in the whole body and it further increased after 4 and 7 months (**Fig. 2A**). Mice sacrificed 10 and 13 months after injection had severe amyloid deposition. In the liver, similar results were observed (**Fig. 2B**).

#### **B Fractionation of soluble and insoluble amyloid fibrils by centrifugation**

We separated soluble and insoluble fractions from liver homogenates (**Fig. 1**). The 3kG-P, 100kG-P, S-3kG-P and S-100kG-P fractions of livers collected 4, 7, and 10 months after injection showed ApoA-II bands (**Fig. 3A**). However, ApoA-II bands were not observed in any of the fractions 2 months after injection (data not shown). The content of ApoA-II was determined by Western blot analysis. The results showed that ApoA-II was mainly contained in the 3kG-P fraction (**Table 1**). After sonication, ApoA-II contents were decreased in the S-3kG-P fraction and increased in the S-100kG-P fraction. Interestingly, sonication of 4m mice liver homogenates increased the contents of ApoA-II in the S-100kG-P fraction to 58.9 % of total ApoA-II. Based on the ThT assay, the fluorescence levels of the amyloid fibrils in 3kG-P, 100kG-P, S-3kG-P, and S-100kG-P fractions did not differ (**Fig. 3B**). We did not detect amyloid fibril-specific fluorescence in the Sol and S-Sol fractions.

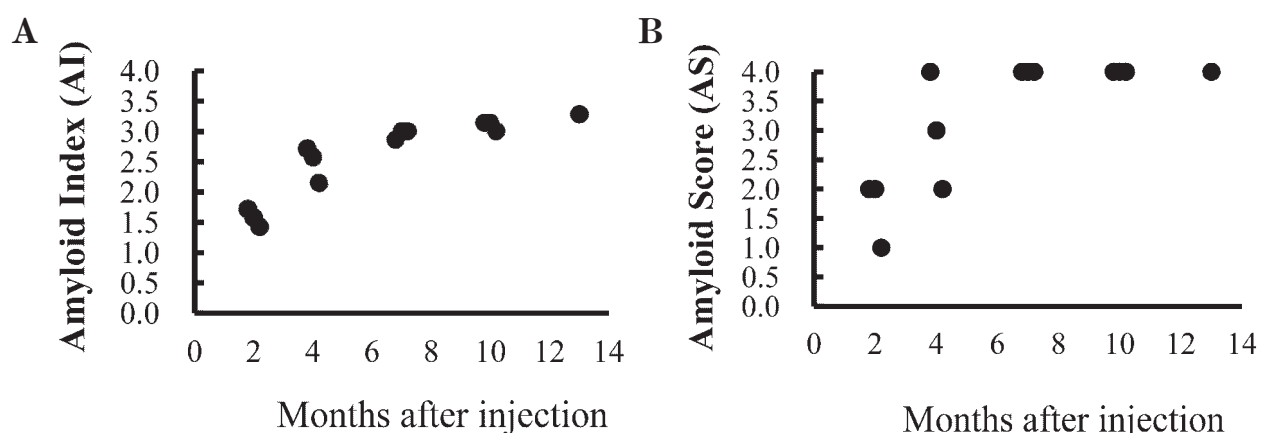


Fig. 2 Amyloid deposition after the induction of amyloidosis. The treated mice were killed after 2, 4, 7, and 10 months (each, n=3) and 13 months (n=1) after induction of amyloidosis. (A) The degree of amyloid deposition in the whole body was compared using the AI. (B) The grade of amyloid deposition in the liver was compared with the AS.

Table 1 Protein and ApoA-II contents in insoluble and soluble fractions without and with sonication (% of total protein and ApoA-II)

Mouse*	Without sonication						With sonication					
	3kG-P		100kG-P		Sol		3kG-P		100kG-P		Sol	
	Protein (%)	ApoAII (%)	Protein (%)	ApoAII (%)	Protein (%)	ApoAII (%)	Protein (%)	ApoAII (%)	Protein (%)	ApoAII (%)	Protein (%)	ApoAII (%)
2m-1												
2m-2	34.2±0.8	a	18.4±2.1	a	47.4±1.6	a	16.1±1.5	a	30.5±2.2	a	53.5±0.9	a
2m-3												
4m-1												
4m-2	34.3±7.7	91.3 <sup>b</sup>	15.3±6.9	8.7 <sup>b</sup>	50.4±5.6	a	14.1±5.8	41.7 <sup>b</sup>	24.9±2.7	58.9 <sup>b</sup>	60.0±5.0	a
4m-3												
7m-1												
7m-2	34.4±4.4	94.1±3.9	11.0±3.5	6.0±3.8	54.5±1.1	a	32.7±1.6	77.5±13.5	17.7±7.3	22.5±13.5	49.6±6.8	a
7m-3												
10m-1												
10m-2	43.8±2.8	98.1±1.1	5.3±0.4	1.9±1.1	50.9±2.9	a	35.4±1.7	69.9±2.9	17.4±1.0	30.1±2.9	42.7±0.8	a
10m-3												

\*The treated mice were killed after 2, 4, 7, and 10 months (each, n=3) and the liver of each mouse was analyzed.

a : no bands were positive for anti-ApoA-II antiserum.

b : the 4m-3 mouse lacked ApoA-II positive bands and figures are means of two mice (4m-1 and 4m-2).

Next, we determined the amyloidosis-inducing activity in the fractions (**Fig. 3C**). Four fractions (3kG-P, 100kG-P, S-3kG-P and S-100kG-P) containing 10  $\mu$ g of ApoA-II protein and Sol and S-Sol fractions (containing 10  $\mu$ g of protein) were injected into the tail veins of 2-month-old R1.P1-*Apoa2<sup>c</sup>* mice (n=3 mice per fraction). The 3kG-P and 100kG-P fractions showed amyloidosis-inducing activity similar to that of standard AApoAII fibrils. After sonication, the amyloidosis-inducing

activity was significantly increased in the S-100kG-P fractions of 10m-1 mice. All the Sol and S-Sol fractions except for Sol of 4m mice showed weak amyloidosis-inducing activity.

To analyze the ultrastructure of the AApoAII in each fraction, we observed negatively stained fibrils using electron microscopy (**Fig. 4**). We observed very small amounts of amyloid fibril-like structures in 3kG-P, 100kG-P, S-3kG-P and S-100kG-P fractions of 4m-1 mice. Abundant amyloid fibrils were

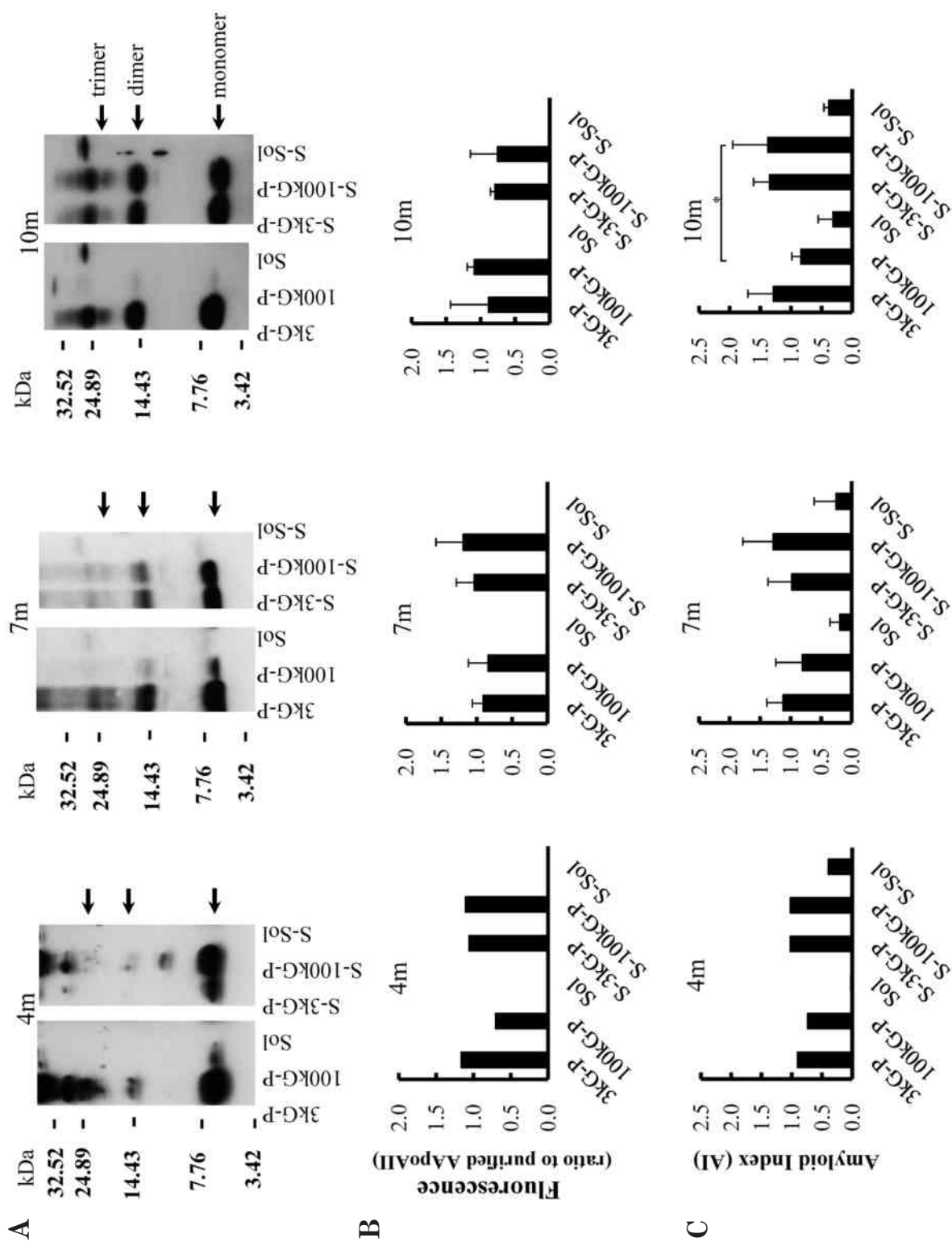


Fig. 3



Fig. 3 ApoA-II in the six soluble and insoluble fractions from the livers of mice. (A) Western blot analysis of the 6 fractions (5  $\mu$ g of protein) obtained from the livers of 4m-1, 7m-1, 10m-1 mice (Table 1) detected with anti-ApoA-II antiserum. Arrows indicate ApoA-II monomer, dimer, trimer. (B) The intensity of amyloid fibril-specific fluorescence per  $\mu$ g of ApoA-II was determined with the ThT binding assay and compared with purified AApoAII amyloid fibrils. (C) Amyloidosis-inducing activity of 6 fractions. Values are means  $\pm$  standard deviation (n=3). \*,  $p < 0.05$  vs. without sonication. Because the 4m-3 mouse showed no ApoA-II-positive bands, figures are means of 2 mice.

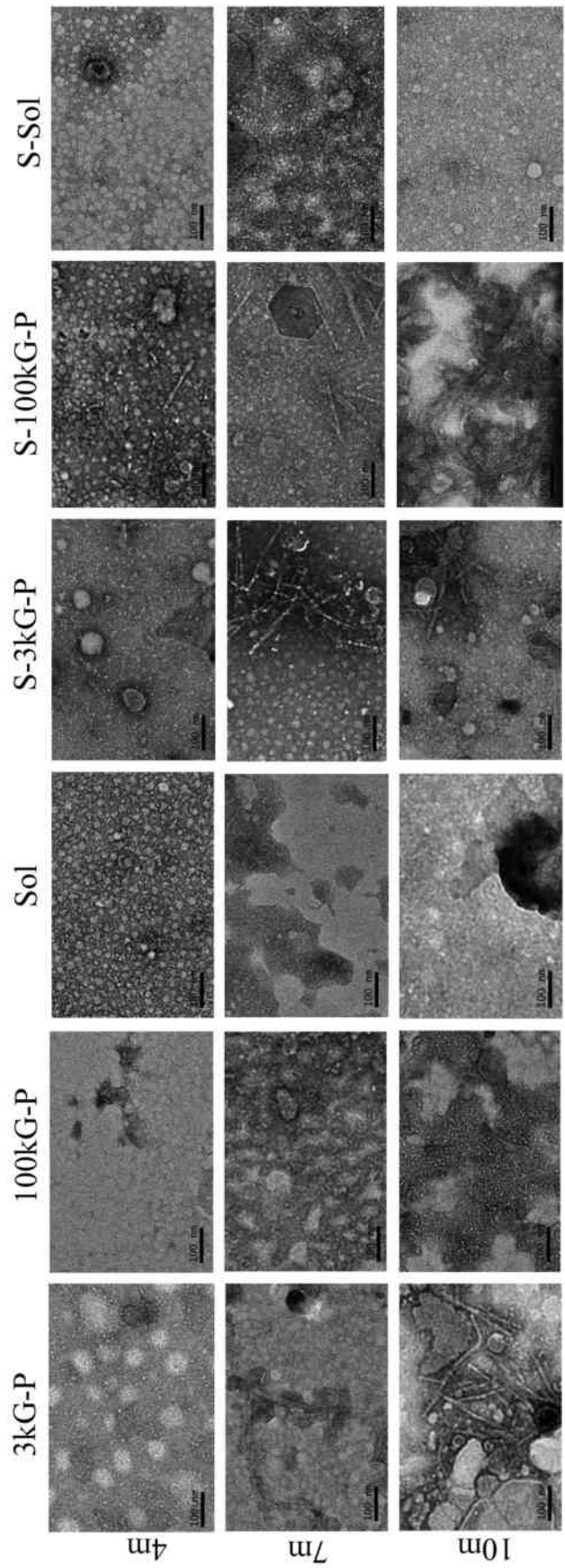


Fig. 4 Transmission electron microscopic images of 6 negatively stained insoluble and soluble fractions of livers. Six fractions from the livers of 4m-1, 7m-1, and 10m-1 mice were observed by transmission electron microscopy. Magnification was X20,000. Scale bars are 100 nm.

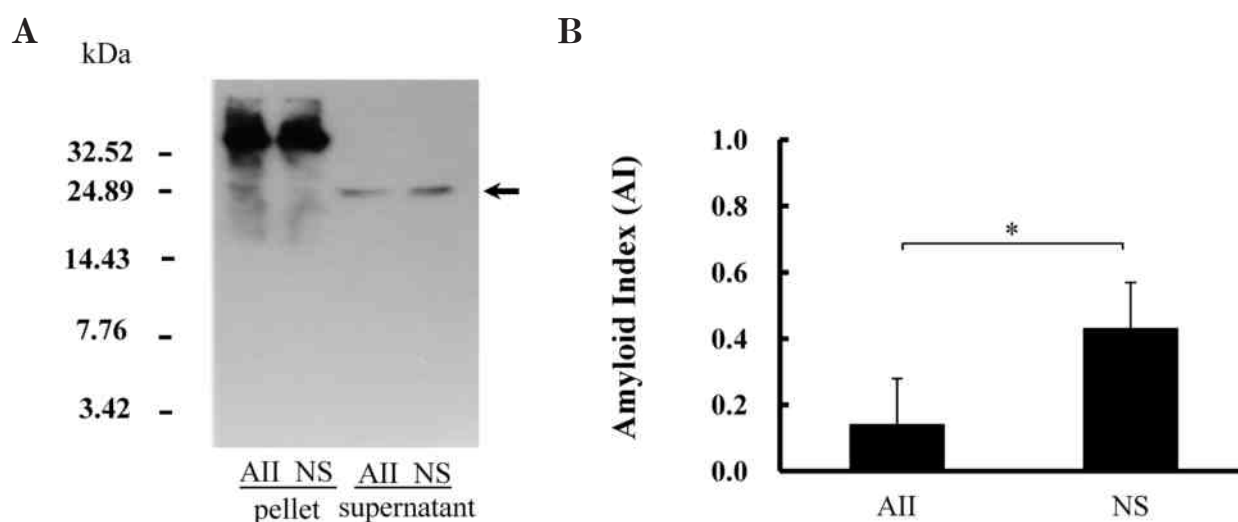


Fig. 5 Immuno-depletion analysis of soluble fractions. The Sol fraction of the 7m-1 mouse was immuno-depleted with anti-ApoA-II antiserum or normal rabbit serum. (A) Western blot analysis of the pellet and supernatant after immuno-depletion. The intensity of  $\sim 25$  kDa protein band of supernatant was reduced after immuno-depletion with anti-ApoA-II antiserum (AII) compared with the band depleted with normal rabbit serum (NS). Arrow indicates  $\sim 25$  kDa bands. (B) Amyloidosis-inducing activity of  $10 \mu\text{g}$  of supernatant protein ( $n=3$  mice per fraction). \*,  $p < 0.05$ .

observed in the 3kG-P fractions of 7m-1 and 10m-1 mice, but only small amounts of smaller amyloid fibril-like structures were found in the 100kG-P fractions of these mice. After sonication, shortened amyloid fibrils were observed in the S-100kG-P fractions in 7m-1 and 10m-1 mice. In contrast, no amyloid fibril-like structures were found in either the Sol or S-Sol fractions.

### C Immuno-depletion analysis of soluble fraction

Soluble fraction of 7m-1 mouse was immuno-depleted with anti-ApoA-II antiserum (Fig. 5). Although ApoA-II monomers could not be detected, bands with a molecular weight of  $\sim 25$  kDa were specifically detected with anti-ApoA-II antiserum. We tried immune-depletion several times with anti-ApoA-II antiserum independently and the intensity of this protein band was reduced to  $\sim 60\%$  ( $0.64 \pm 0.13$ ,  $n=4$ ) of the band depleted with normal rabbit serum, but did not disappear completely (Fig. 5A, right two lanes). We next determined the amyloidosis-inducing activity of immuno-depleted soluble fractions. The fractions immuno-depleted with anti-ApoA-II antiserum showed weaker amyloidosis-inducing activity than that in a fraction depleted with normal rabbit serum (Fig. 5B).

### D Fractionation of amyloid fibrils with non-denaturing PAGE

Four, 7, 10 and 13 months after the induction of amyloidosis, AApoAII fibrils were isolated from the livers<sup>19</sup>. We analyzed the extent of polymerization of ApoA-II in AApoAII fibrils with non-denaturing PAGE. Specifically, the distribution of monomers, dimers, trimers, tetramers, pentamers, small oligomers, large oligomers and fibrils was determined. The distribution patterns of these assemblies did not change with the progression of amyloidosis (Fig. 6A). At 4, 7 and 10 months, five fractions (I-V) were cut out from PAGE gels as judged by their molecular weights. The proteins were extracted from the 5 gel fractions and assessed for amyloid fibril-specific fluorescence with the ThT binding assay. The fluorescence of each fraction was very low. Those results suggested that ApoA-II proteins in each fraction did not have a  $\beta$ -pleated structure (Fig. 6B). To assess the amyloidosis-inducing activity, fractions were injected into the tail veins of R1. P1-*Apoa2*<sup>c</sup> mice. All 5 of the fractions showed weak transmission activity (Fig. 6C).



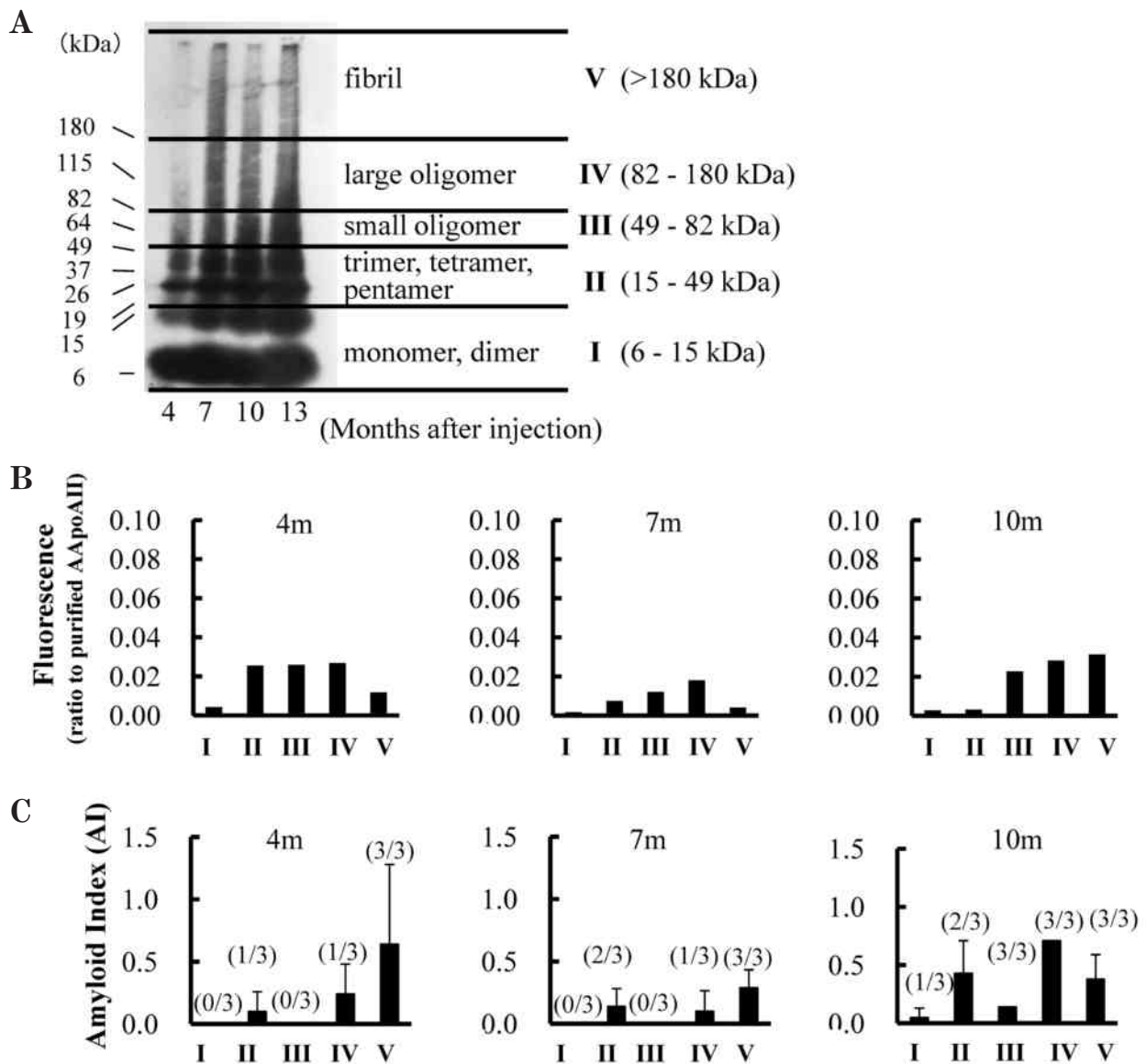


Fig. 6 Non-denaturing PAGE analyses of AApoAII amyloid fibrils. (A) AApoAII amyloid fibrils were isolated from the livers of 4m-1, 7m-1 and 10m-1 and 13m-1 mice. AApoAII amyloid fibrils were analyzed with non-denatured PAGE and Western blot analysis. The distribution of monomers, dimers, trimers, tetramers, pentamers, small oligomers, large oligomers and fibril was determined. Fraction I (monomers and dimers), II (trimers, tetramers and pentamers), III (small oligomers), IV (large oligomers) and V (fibrils) were cut out and the proteins were extracted from the gels. (B) The intensity of amyloid fibril-specific fluorescence per  $\mu\text{g}$  of protein in each fraction isolated from 4m-1, 7m-1 and 10m-1 mice was determined by the ThT binding assay. (C) Amyloidosis-inducing activity of each fraction ( $10 \mu\text{g}$  protein) was determined ( $n=3$  mice per fraction). Figures in parentheses represent number of amyloid-positive mice/number of mice examined.

#### IV Discussion

In the studies of brain samples of AD patients, the size of the soluble pools consisting of small  $A\beta$  aggregates was highly correlated with the severity and progression of AD<sup>22</sup>). Thus, we studied the

distribution and transmissibility of AApoAII in insoluble and soluble fractions of the liver in which different amounts of amyloid were deposited. Six fractions were isolated from the liver by homogenization and centrifugation (**Table 1**). Determination of ApoA-II contents in each fraction revealed that

over 90 % of ApoA-II was contained in the 3kG-P fractions of the liver homogenates regardless of whether deposition was light (4 months after induction) or heavy (10 months after injection). After sonication, the ApoA-II content was decreased in the S-3kG-P fraction and increased in the S-100kG-P fraction. Abundant amyloid fibrils were observed in the 3kG-P fractions. However, they were rarely found in 100kG-P fractions. After sonication, shortened amyloid fibrils were observed in the S-100kG-P fractions. Sonication might break AApoAII amyloid fibrils in the 3kG-P fraction and fragmented fibrils might be fractionated into the S-100kG-P fraction. Amyloidosis-inducing activity of the S-100kG-P fraction from the 10m-1 mouse was significantly higher than that of the 100kG-P fraction (**Fig. 3C**). It was reported that sonicated prions and A $\beta$  fibrils in brain homogenates had increased seeding potentials after fragmentation of fibrils into smaller, soluble species by increasing the active site of fibrils<sup>17)23)24)</sup>.

The ThT binding assay quantitates AApoAII amyloid fibrils with high sensitivity and specificity<sup>20)</sup>. In our previous work, many denaturing treatments partially disrupted amyloid fibril structure and there was a distinct correlation between the fluorescence determined with the ThT binding assay and amyloidosis-inducing activity. Those results suggested that the structure of amyloid fibrils might be important for induction of amyloidosis<sup>25)</sup>. The fluorescence levels in ThT binding assays did not differ among 3kG-P, 100kG-P, S-3kG-P and S-100kG-P fractions and were about the same as purified AApoAII fibrils (**Fig. 3B**). The molecular structure to which ThT binds is still not clear. Thus, we do not know whether ApoA-II proteins in 3kG-P, 100kG-P, S-3kG-P and S-100kG-P fractions showed similar fluorescence and had the same molecular structure, although the electron microscopic structures were clearly different.

We had speculated that the composition of amyloid-associated molecules such as apolipoprotein E and heparin sulfate proteoglycan might change during the progression of amyloidosis and

thereby modify the structure of ApoA-II amyloid protein. We did not observe the effects of progression of amyloid deposition in the liver on the biochemical characteristics including transmission activity of amyloid fibrils.

All the Sol and S-Sol fractions showed weak amyloidosis inducing activity (**Fig. 3C**). We did not detect ApoA-II proteins in our Western blot analysis nor did we find any amyloid fibril-like structures in electron microscopic examination of the Sol and S-Sol fractions (**Fig. 4**). In the mouse model of AD, very small amounts of soluble A $\beta$  with higher amyloidosis-inducing-activity might mediate the spread of A $\beta$  amyloidosis<sup>17)</sup>. We detected bands reactive with anti-ApoA-II antiserum in the Sol fraction (**Fig. 5**), in immuno-depletion analysis, we estimated a molecular weight of ~25 kDa. This ~25 kDa band was also detected in Sol and S-Sol fractions of 7m and 10m mice (**Fig. 3A**). Reduction of this band by immuno-depletion with ApoA-II antiserum decreased amyloidosis-inducing activity. We will characterize these bands in future studies.

In studies of prion disease, it was found that prions existed in a range of sizes and that nonfibrillar small particles were the most infectious agents<sup>13)</sup>. We used non-denaturing PAGE to characterize multiple ApoA-II assemblies of AApoAII amyloid fibrils that had been extracted from the livers. The AApoAII amyloid fibrils contained multiple AApoAII assemblies from monomers to fibrils. We cut out sections (fractions I-V) from the non-denaturing PAGE (**Fig. 6**). We found that ApoA-II assemblies in fractions I-IV had very small amounts of amyloid fibril-specific fluorescence and that they had only slight activity for amyloid induction. Thus, the specific amyloidosis-inducing activity per ApoA-II monomer of fractions I-IV was low compared with purified AApoAII fibrils. In general, fraction V was very difficult to extract from the gels due to their high molecular weights. It is possible that only degraded fibrils were extracted and did not show high inducing activity. From these findings, we postulate that the partially purified AApoAII amyloid fibrils isolated from the livers

contained multiple ApoA-II assemblies from monomers to large oligomers. However, these assemblies had only a slight  $\beta$ -pleated structure and a low amyloidosis-inducing activity. We will characterize these multiple assemblies using other isolation methods in future studies.

The results above suggest that multiple ApoA-II assemblies exist as insoluble molecules. Their characteristics, including amyloidosis-inducing activity, do not change with the progression of amyloidosis. We cannot deny the possibility that very small amounts of soluble ApoA-II with higher amyloidosis-inducing activity mediate the transmission of amyloidosis. However, we have found AApoAII amyloid fibrils in feces, milk, muscle and saliva<sup>7)8)</sup>, and the fibrils possessed amyloidosis-inducing activity. Thus, we believe that amyloid fibrils are

quite important inducers in the transmission of AApoAII amyloidosis.

## V Declaration of Interest

The authors declare no conflicts of interest. This research was supported by Grants-in-Aid for Scientific Research (B) 23390093 and 26293084, and Challenging Exploratory Research 26670152 from the Ministry of Education, Culture, Sports, Science, and Technology of Japan and by grants from the Intractable Disease Division, the Ministry of Health, Labor, and Welfare to the Research Committees for Amyloidosis. We thank Drs. Kiyoshi Matsumoto, Yoshizawa Takahiro and Ms. Kayo Suzuki (Research Center for Human and Environmental Science, Shinshu University) for the care of mice and technical assistance.

## References

- 1) Merlini G, Bellotti V : Molecular mechanisms of amyloidosis. *N Engl J Med* 349 : 583-596, 2003
- 2) Sipe JD, Benson MD, Buxbaum JN, Ikeda S, Merlini G, Saraiva MJ, Westermark P : Nomenclature : Amyloid fibril proteins and clinical classification of the amyloidosis. *Amyloid* 21 : 221-224, 2014
- 3) Jucker M, Walker LC : Pathogenic protein seeding in Alzheimer disease and other neurodegenerative disorders. *Ann Neurol* 70 : 532-540, 2011
- 4) Higuchi K, Yonezu T, Kogishi K, Matsumura A, Takeshita S, Kohno A, Matsushita M, Hosokawa M, Takeda T : Purification and characterization of a senile amyloid-related antigenic substance (apoSASSAM) from mouse serum. apoSASSAM is an apoA-II apolipoprotein of mouse high density lipoproteins. *J Biol Chem* 261 : 12834-12840, 1986
- 5) Higuchi K, Naiki H, Kitagawa K, Kitado H, Kogishi K, Matsushita T, Takeda T : Apolipoprotein A-II gene and development of amyloidosis and senescence in a congenic strain of mice carrying amyloidogenic ApoA-II. *Lab Invest* 72 : 75-82, 1995
- 6) Benson MD, Liepnieks JJ, Yazaki M, Yamashita T, Hamidi Asl K, Guenther B, Kluge-Beckerman B : A new human hereditary amyloidosis : the result of a stop-codon mutation in the apolipoprotein AII gene. *Genomics* 72 : 272-277, 2001
- 7) Xing Y, Nakamura A, Chiba T, Kogishi K, Matsushita T, Li F, Guo Z, Guo Z, Hosokawa M, Mori M, Higuchi K : Transmission of mouse senile amyloidosis. *Lab Invest* 81 : 493-499, 2001
- 8) Qian J, Yan J, Ge F, Zhang B, Fu X, Tomozawa H, Sawashita J, Mori M, Higuchi K : Mouse senile amyloid fibrils deposited in skeletal muscle exhibit amyloidosis-enhancing activity. *PLoS Pathog* 6 : e1000914, 2010
- 9) Aguzzi A, Heikenwalder M, Polymenidou M : Insights into prion strains and neurotoxicity. *Nat Rev Mol Cell Biol* 8 : 552-561, 2007
- 10) Collinge J, Clarke AR : A general model of prion strains and their pathogenicity. *Science* 318 : 930-936, 2007
- 11) Masel J, Genoud N, Aguzzi A : Efficient inhibition of prion replication by PrP-Fc (2) suggests that the prion is a PrP (Sc) oligomer. *J Mol Biol* 345 : 1243-1251, 2005
- 12) Fichet G, Comoy E, Duval C, Antloga K, Dehen C, Charbonnier A, McDonnell G, Brown P, Lasmézas CI, Deslys

- JP : Novel methods for disinfection of prion-contaminated medical devices. *Lancet* 364 : 521-526, 2004
- 13) Silveira JR, Raymond GJ, Hughson AG, Race RE, Sim VL, Hayes SF, Caughey B : The most infectious prion protein particles. *Nature* 437 : 257-261, 2005
  - 14) Haass C, Selkoe DJ : Soluble protein oligomers in neurodegeneration : lessons from the Alzheimer's amyloid  $\beta$ -peptide. *Nat Rev Mol Cell Biol* 8 : 101-112, 2007
  - 15) Mc Donald JM, Savva GM, Brayne C, Welzel AT, Forster G, Shankar GM, Selkoe DJ, Ince PG, Walsh DM : The presence of sodium dodecyl sulphate-stable A $\beta$  dimers is strongly associated with Alzheimer-type dementia. *Brain* 133 : 1328-1341, 2010
  - 16) McLean CA, Cherny RA, Fraser FW, Fuller SJ, Smith MJ, Beyreuther K, Bush AI, Masters CL : Soluble pool of A $\beta$  amyloid as a determinant of severity of neurodegeneration in Alzheimer's disease. *Ann Neurol* 46 : 860-866, 1999
  - 17) Langer F, Eisele YS, Fritschi SK, Staufenbiel M, Walker LC, Jucker M : Soluble A $\beta$  seeds are potent inducers of cerebral  $\beta$ -amyloid deposition. *J Neurosci* 31 : 14488-14495, 2011
  - 18) Eisele YS, Fritschi SK, Hamaguchi T, Obermuller U, Fuger P, Skodras A, Schafer C, Odenthal J, Heikenwalder M, Staufenbiel M, Jucker M : Multiple factors contribute to the peripheral induction of cerebral  $\beta$ -amyloidosis. *J Neurosci* 34 : 10264-10273, 2014
  - 19) Xing Y, Nakamura A, Korenaga T, Guo Z, Yao J, Fu X, Matsushita T, Kogishi K, Hosokawa M, Kametani F, Mori M, Higuchi K : Induction of protein conformational change in mouse senile amyloidosis. *J Biol Chem* 277 : 33164-33169, 2002
  - 20) Naiki H, Higuchi K, Hosokawa M, Takeda T : Fluorometric determination of amyloid fibrils in vitro using the fluorescent dye, thioflavin T. *Anal Biochem* 177 : 244-249, 1989
  - 21) Higuchi K, Matsumura A, Honma A, Takeshita S, Hashimoto K, Hosokawa M, Yasuhira K, Takeda T : Systemic senile amyloid in senescence-accelerated mice. A unique fibril protein demonstrated in tissues from various organs by the unlabeled immunoperoxidase method. *Lab Invest* 48 : 231-240, 1983
  - 22) Tomic JL, Pensalfini A, Head E, Glabe CG : Soluble fibrillar oligomer levels are elevated in Alzheimer's disease brain and correlate with cognitive dysfunction. *Neurobiol Dis* 35 : 352-358, 2009
  - 23) Knowles TP, Waudby CA, Devlin GL, Cohen SI, Aguzzi A, Vendruscolo M, Terentjev EM, Welland ME, Dobson CM : An analytical solution to the kinetics of breakable filament assembly. *Science* 326 : 1533-1537, 2009
  - 24) Brachmann A, Baxa U, Wickner RB : Prion generation in vitro : amyloid of Ure2p is infectious. *EMBO J* 24 : 3082-3092, 2005
  - 25) Zhang H, Sawashita J, Fu X, Korenaga T, Yan J, Mori M, Higuchi K : Transmissibility of mouse AApoAII amyloid fibrils : inactivation by physical and chemical methods. *FASEB J* 20 : 1012-1014, 2006

(2016. 2. 9 received ; 2016. 2. 25 accepted)